42nd AIAA Aerospace Sciences Meeting and Exhibit
5 - 8 January 2004, Reno, Nevada

AIAA 2004-527

Recent Improvements to the Wind(-US) Code at AEDC*

C. C. Nelson †
D. W. Lankford †
Aerospace Testing Alliance
Arnold Engineering Development Center
Arnold Air Force Base, TN 37389

R. H. Nichols†
University of Alabama at Birmingham
DoD PET Program/AEDC
Arnold Engineering Development Center
Arnold Air Force Base, TN 37389

Development of the Wind code did not stop with the release of version 5.0 in mid 2002. Several important new capabilities have been added recently. Among these additions are a second-order, implicit-time marching algorithm, new hybrid turbulence models, and improvements to the SST turbulence models. Many of the recent changes have been focused on improving Wind's ability to run time-accurate cases. Other work has focused on the addition of multi-phase particle tracking to the code. Other changes have not so much added new capabilities as made existing ones more reliable. This paper reports on the progress of this activity and presents sample applications that make use of some of the improved capabilities.

Introduction

Version 1.0 of the Wind code was introduced in 1997 by the NPARC Alliance as a replacement for the venerable NPARC code.[1] Wind was based on the NASTD solver,[2] which was donated by Boeing to the NPARC Alliance. Since then four additional versions have been released, bringing the current production version number to 5.0. Each of these versions has shown substantial improvements[3–5] over prior releases. Recently, Boeing donated an unstructured flow solver to the NPARC Alliance for incorporation into the Wind solver. With such a major technology addition, it has been decided to rename the code Wind-US. Thus, what would have been Wind version 6.0 will now be Wind-US version 1.0. While the addition of an unstructured solver is a significant development, and a great deal of the integration work has been performed at the Arnold Engineering Development Center (AEDC), the current paper focuses on improvements to Wind-US that originated at AEDC. The unstructured solver will be documented in a future paper.

Development of Wind-US is loosely coordinated by the NPARC Alliance and is open to anyone who is entitled to run the code. Each contributor works on the items of most interest to them. The NPARC Alliance members decide among themselves whether or not to include any changes submitted for inclusion in the official version.

In practice, the majority of the development takes place at three locations: Boeing Phantom Works at Saint Louis, NASA's Glenn Research Center, and AEDC. Currently, Boeing's major emphasis is on the development of an unstructured/hybrid capability. NASA Glenn is developing improved RANS turbulence modeling capabilities and a vortex generator model. At AEDC, most of the development work involves extending and improving the structured flow solver. Areas of particular interest at AEDC include unsteady flows (including turbulence modeling) and reacting flows (including multi-phase cases with reacting particles convected by the flow).

A significant fraction of the CFD applications performed at AEDC involve time-accurate simulations of aircraft store drops. These simulations have typically been performed with the NXAIR solver,[6] but the NPARC Alliance has always had the goal of being able to do the same thing with its CFD solver. Toward that end, several technologies have been added to the code over the years. These include Newton iterations, the HLLE flux-difference splitting algorithm, double-fringe overlapped boundaries, Gauss-Seidel and Jacobi implicit solvers, and the time-step calculation algorithm from OVERFLOW[7] (which is similar to that used in NXAIR). As of version 5 of Wind, the major remaining difference between it and NXAIR was the lack of a second-order, implicit time-marching algorithm. This has now been added. In addition, a new hybrid turbulence model has been implemented that seeks to combine the best features of traditional Reynolds-averaged Navier-Stokes (RANS) models with the strengths of Large Eddy Simulation (LES) approaches. The Menter Shear Stress Transport (SST) model has also been upgraded to include terms which model the effects of compressibility.

*The research reported herein was performed by the Arnold Engineering Development Center AEDC, Air Force Materiel Command. Work and analysis for this research were performed by personnel of Aerospace Testing Alliance, technical services contractor for AEDC. Further reproduction is authorized to satisfy needs of the U.S. Government

†Senior Member AIAA

This paper is a work of the U.S. Government and is not subject to copyright protection in the United States.

This material is declared a work of the U.S. Government and is not subject to copyright protection in the United States.

A variety of multiphase flow analysis applications have arisen at AEDC in the recent past that were not readily addressable with current capabilities. These include spray combustion in the APTU facility, jet exhaust quenching in the T6 engine test facility, and aircraft icing in the ASTF facility. There are also a number of applications in the space and missiles area that could benefit from an easy to use, well-supported analysis tool. For a variety of reasons, mostly involving codes being either unavailable or unsupported, the available resources at AEDC for multiphase simulations were deemed inadequate. Since Wind (and soon Wind-US) has a broad user base, and the NPARC Alliance is committed to supporting the code, it was decided to use Wind-US as the foundation on which to build a multiphase capability.

In addition to the above "major" new features, there have been many smaller additions to the code. Also, many preexisting capabilities have been significantly revamped in order to improve their reliability and maintainability. In the following sections, the various fixes and improvements are discussed, and some sample applications are presented to showcase the new options.

Second-Order Implicit Time Marching

As discussed above, one of the factors which has limited Wind-US's applicability in the realm of unsteady flows has been the implicit time-marching procedure. The default algorithm which came from NASTD was a first-order backward Euler scheme. This scheme is unsuited to time-accurate simulations, and, indeed, it was never intended to be used in such a fashion. In NASTD, unsteady simulations always used one of the available Runge-Kutta explicit time-marching procedures.

With Wind-US, however, one of the objectives was to be able to perform store-drop simulations in an efficient manner. This requires the ability to run time-accurate simulations of complex geometries with very large time steps, and this necessitates an implicit algorithm. Thus, an implicit procedure for time-accurate simulations has been of interest from the beginning.

To illustrate the problems with the original implicit time-marching algorithm in Wind, a simple inviscid vortex convection case has been run. This case was obtained from the suite of test cases that are distributed with the OVERFLOW solver. A vortex in a uniform mean flow is simulated on a uniform 80x80 Cartesian grid (not including boundary points) covering 10 ft on each side. The boundary conditions are periodic so that as the vortex is swept out the back of the domain, it reappears at the inflow. The freestream Mach number was 0.5, the total temperature was 525°R, and the total pressure was 0.937 psi. A nondimensional time step of 0.1 was used, which translates to a dimensional step of 9.124×10^{-5} sec and 200 time steps per flow-through time. The default second-order Roe spatial scheme and ADI matrix inversion algorithms were employed.

Figure 1 shows density contours for both the initial conditions and after five flow-through times. From the figure, it is obvious that the default scheme is inappropriate for unsteady time marching. By the end of five flow-through times, significant dissipation and dispersion errors are present.

As a first step toward improving the unsteady implicit capability, a Newton iteration procedure was added relatively early on in the process of developing Wind. This improved the time-marching ability, but persistent problems were present in the implementation and have only recently been resolved. Figure 2 shows the results for the same test case using Newton iterations in conjunction with the first-order, time-marching algorithm. For this case, five subiterations were used at each time level. The addition of Newton iterations reduces the dispersion error considerably, but the dissipation in the scheme is still unacceptably large.

A second-order implicit time-marching algorithm has now been implemented. This technique is applicable either with or without Newton iterations. At present, all of the implicit schemes in Wind, except for the MacCormack implicit scheme, can be used with this second-order capability. Figure 3 shows results for the same case using the second-order scheme without any Newton iterations. As the figure clearly shows, the dissipation is greatly reduced, but the dispersion error is still unacceptably large.

Finally, a run was performed using the second-order algorithm with Newton iterations. Again, five subiterations were used at each time level. Figure 4 shows the resulting density contours. In this case, not only has the dissipation been dramatically reduced by the second-order scheme, compared to the first order algorithm, but the Newton iteration procedure has dramatically reduced the dispersion error. This result, while still more dissipative than the high-resolution schemes typically used for the most demanding unsteady simulations, is clearly a significant improvement over the original algorithm in Wind.

Hybrid Turbulence Model

Another limiting factor for unsteady flow simulations is the fact that most turbulence models have been designed for steady-state flows. When such models are applied in unsteady situations, they are often too dissipative, damping out features that should be resolved. Various techniques have been developed recently to mitigate this problem. Within Wind, both the Detached Eddy Simulation (DES) model of Spalart[8] and the LESb model of Bush[9] have been available for some time. Recently a third such option has been implemented.

The hybrid RANS/LES turbulence model technique of Nichols and Nelson[10] has been added to both the SST and Chien $k-\varepsilon$ models. This model has been found to be as good as DES in many cases and offers some advantages in others.[11,12] This technique takes a somewhat different approach than the more common DES model. First, standard RANS turbulence model equations are solved to predict the overall turbulence in the flow field. Next, an estimate is made as to what fraction of that turbulence is being re-

solved on the computational grid and how much must be modeled. Finally, this estimate is used to compute the turbulent viscosity that is employed in the solution of the Navier-Stokes equations. In practice, extending a RANS turbulence model to use this hybrid technique is a straightforward matter of modifying the eddy viscosity calculation:

$$\nu_t = \Lambda \nu_{t_{RANS}} + (1 - \Lambda)\, \nu_{t_{LES}} \tag{1}$$

In the above equation, the "LES" eddy viscosity ($\nu_{t_{LES}}$) is computed on the basis of a form taken from an LES k-equation model:[13]

$$\nu_{t_{LES}} = \min\left(c_{\mu_{LES}} \Delta \sqrt{k_{LES}},\, \nu_{t_{RANS}}\right) \tag{2}$$

For the current work, a value of 0.0854 was used for the LES model coefficient ($c_{\mu_{LES}}$). The subgrid (LES) turbulent kinetic energy is defined in terms of the RANS model's prediction for turbulent kinetic energy as:

$$k_{LES} = f_d k_{RANS} \tag{3}$$

where the clipping function is defined as a function of the predicted turbulent length scale and the local grid size:

$$f_d = \frac{1}{1 + \left(\frac{l_2}{2\Delta}\right)^{\frac{4}{3}}} \tag{4}$$

It should be noted that the question of whether or not the factor of '2' should appear in front ofΔ in the above equation has not been finally resolved, and the current implementation in the NXAIR code does have it. The turbulent length scale used in this effort is defined by

$$l_t = \max\left(6\sqrt{\frac{\nu_{t_{RANS}}}{\omega}},\, \frac{k_{RANS}^{\frac{3}{2}}}{\varepsilon_{RANS}}\right) \tag{5}$$

This length scale is a mixture of the traditional turbulent scale definition for two-equation turbulence models ($k^{3/2}/\varepsilon$) and the definition usually associated with algebraic turbulence models ($\sqrt{\nu_t/\omega}$). The factor of six was chosen, such that the two components of the length scale were approximately equal in a simple test case. This turbulent length scale definition could be easily adapted to other types of turbulence models. The cut-over function (Λ) in Eq. (1) is defined as:

$$\Lambda = \frac{1}{2}\left(1 + \tanh\left(2\pi\left(f_d - \frac{1}{2}\right)\right)\right) \tag{6}$$

In practical terms, then, this hybrid model for unsteady turbulent flows can be described as filtering the RANS turbulence models such that the eddy viscosity does not include the energy of grid-resolved turbulent scales. Therefore, the filtered RANS turbulence model may be thought of as a subgrid model for very large turbulent eddies. The objective in choosing the filter function is that it should not degrade the performance of the turbulence model when the largest turbulent scales present are below the resolution of the grid, as is generally the case in current aircraft CFD applications–certainly the case near viscous walls, and often so elsewhere. This approach should be viable for the current class of CFD flow solvers and would not require any more grid resolution than is already used for steady-state simulations, except in areas where finer details of the instantaneous flow structures are desired.

The implementation of this model into Wind is still fairly recent. Therefore, very few results are currently available to show its capability. One case that has been run is an unsteady simulation of the vortices shed behind a two-dimensional circular cylinder. The reference Mach number was 0.2, and the Reynolds number based on cylinder diameter was 8×10^6. The computational grid was 201×201 with an initial wall spacing of 2×10^{-4}diameters, which corresponds to a y^+ of about 20. Wall function boundary conditions were employed, and the solution was marched in time at a constant time step of about 3×10^{-4} sec, which corresponds to about 150 steps per cycle of the shedding frequency.

Figure 5 shows the nondimensional pressure for this case when it is run using a conventional Menter SST model. The results using the new hybrid model (with the SST model as the base) are shown in Fig. 6. Compared to the baseline model, the hybrid results are showing much more fine scale details of the flow, particularly in the vicinity of the separation points. This is at least qualitatively in accordance with expectations. Of course, since real turbulence is always three dimensional, one must be careful in drawing conclusions about turbulence models based on the results of a two-dimensional case such as this one.

Compressible Version of SST Turbulence Model

A second version of the SST turbulence model has been added to the code. This version is implemented in conservative form and includes the compressibility corrections of Suzen and Hoffmann.[14] This is expected to greatly aid in the simulation of free shear layers at transonic speeds (and higher) and other flows where the effects of compressibility are expected to be significant. The compressibility corrections include a pressure dilatation model and a turbulent Mach number based model of compressible dissipation.

To demonstrate the effect of the various changes to the SST model, a simple axisymmetric jet case was performed. This case involves a "submerged" turbulent supersonic jet emanating from an axisymmetric convergent-divergent Mach 2.2 nozzle. This nozzle was first studied by J. M. Eggers in 1962.[15] The working fluid was air, and the nozzle was operated at the pressure ratio corresponding to perfect expansion. The nozzle plenum conditions were set to a total temperature of $525°$R , and the total pressure was 162.2psia. The ambient temperature was $252°$R , and the ambient pressure was 14.7psia.

The simulated centerline axial velocity is plotted in Fig.

7 for four different cases as well as the experimental data of Eggers. The first two curves on the plot (designated SST1 and SST2 on the legend) lie on top of each other. They are for the original version of the SST model and the new conservative version with no compressibility corrections added. As expected, they are overly dissipative of the velocity downstream of the potential core. The curve designated "SST2-CD" shows the effect of the compressible dissipation correction, while the curve labeled "SST2-CD-PD" shows the same case with pressure dilatation and compressible dissipation added in. With the addition of the compressibility corrections, the velocity decay is much better predicted aft of the potential core, but the length of the potential core is increasingly over-predicted. This is in line with the observations of other researchers.[16] Thus, this capability, while helpful in some cases, must be used with caution.

Improved Inflow Boundary Condition

In an interior flow case, it is often convenient to specify total conditions at an inflow boundary. In the course of FY2003, a user of the Wind code reported problems in using the "hold totals" inflow boundary condition. As a result of this problem, the inflow condition was rewritten in a greatly improved form that is both more stable and more accurate than the previous version. While this project did fund for that work, it does stand to benefit from it, and thus a brief overview is presented.

The idea of both the old and the new boundary conditions is the same. The user specifies a total temperature, total pressure, and flow angle at the boundary (which can vary from point to point). These quantities are held fixed while the R_2 Riemann invariant ($u_\perp - \frac{2c}{\gamma-1}$) is extrapolated from the interior. The previous implementation, however, used a Newton iteration to simultaneously solve for the temperature and velocity at the boundary point. The new implementation first solves a quadratic equation for the speed of sound based on substituting the normal velocity between the T_0 and R_2 equations. This yields the temperature, and the velocity can then be found from the definition of R_2.

The new approach is generally the same as that taken in the OVERFLOW code.[17] In Wind-US, however, the Riemann invariant is extrapolated to the boundary using a first order algorithm, rather than the more usual zeroth order. This seemingly simple change makes a noticeable improvement in the total pressure distribution interior to the boundary, as shown in Fig. 8 for a representative duct case. It is especially telling that one cannot even obtain a converged answer at all using the old boundary conditions unless one sets up the flow with some other inflow boundary treatment, whereas the new conditions are stable enough to be used from the start. As is typical of characteristic-based boundary conditions, there are fluctuations in the total conditions immediately downstream of the boundary. With the new implementation, however, the values eventually return to the freestream conditions, whereas with the previous boundary conditions (and indeed the new implementation as well, unless a first-order extrapolation of the invariant is used) the flow never returns to the freestream conditions. This is illustrated in Fig. 9, which shows the normalized total pressure along the center line. Considering that Wind-US is currently a single precision code, it would appear unlikely that further significant improvements are possible without first addressing the precision issue.

Multiphase Model

The multiphase algorithms which have been added to Wind-US are based on those used in KIVA. The KIVA codes were developed at Los Alamos for reciprocating engines with fuel spray injection. KIVA has been widely used for engine analysis, but it is difficult to apply to more general problems.

Because of distinct differences between the KIVA and the Wind-US flow models, substantial adaptation and reprogramming were required to incorporate the KIVA particle model into Wind-US. For example, KIVA is a cell-centered, dual mesh, arbitrary Lagrangian-Eulerian flow solver, while Wind-US is a node-centered Eulerian flow solver. This results in a number of geometry-related differences. Also, KIVA computations are performed in CGS units while Wind-US generally performs internal computations using nondimensional variables. This requires rewriting particle models in terms of nondimensional variables. In addition, the numerical coupling of gas phase source terms has been modified.

The multiphase version of Wind-US has been designed for a wide range of cases. For example, liquid or solid particles may be injected. Also, evaporation, two-way gas/particle coupling, and gravity may be included or excluded. Nozzles may be included as sets with similar characteristics. Since Wind-US performs gas phase chemical reactions, the multiphase version should be capable of computing simplistic gas phase spray combustion. As is generally the case, particle drag, diffusion, heat transfer, and mass transfer are computed from model equations rather than first principles. If desired, however, alternate models can be implemented with relative ease. One notable limitation to the current implementation is that the void fraction is not included in the particle model. Therefore, dense particle flow cannot be computed accurately.

To demonstrate the multiphase capability, a simple test case was constructed. This case consists of a single nozzle injecting particles into Mach 4 flow over a ramp. The grid is split into two zones for this case. Figure 10 shows a snapshot of the particle positions in the upstream zone. Figure 11 shows the particle accumulation over time at the outflow plane.

Method of Manufactured Solutions and Rusanov Scheme

The Method of Manufactured Solutions (MMS) is a technique by which numerical methods within codes can be verified to ensure that they have been coded correctly

and do, in fact, solve the equations that they claim to solve. While the basic ideas of MMS were developed some time ago,[18–20] MMS has only recently begun to be applied to large, general-purpose flow solvers. The procedure for applying MMS to a code is as follows:

- Choose the form of the governing equations (typically functions of sines and cosines)
- Chose the form of the manufactured solution
- Apply the governing equations to the manufactured solution to generate analytical source terms
- Solve the equations on multiple mesh levels using the source terms
- Evaluate the global discretization error in the numerical solutions
- Determine the order of accuracy

If the order of accuracy matches the theoretical value, then the portions of the code that were tested can be considered verified.

Within Wind-US, MMS has been used to verify a fairly broad selection of both new and old options. Here, the discussion is confined to only the new Rusanov scheme for computing the explicit inviscid fluxes. More details on MMS and its application to Wind-US are found in Ref 21.

One of the algorithms used on the right-hand side of the unstructured portion of Wind-US to compute inviscid fluxes is the Rusanov scheme.[22] For the unstructured solver, this relatively simple algorithm was found to be both robust and accurate, but it was originally not implemented in the structured solver. To enable grids with both structured and unstructured zones to be run with a consistent algorithm, the Rusanov scheme was implemented for the structured code as well. MMS was then used to test the scheme. The test looked at the third-order upwind-biased extrapolation algorithm on a uniform 2-D Cartesian grid. The code was run in inviscid mode to prevent the second-order viscous terms from corrupting the results. The manufactured solution was purely subsonic, and the exact solution was applied on the boundaries in lieu of regular boundary conditions. Results were obtained for seven resolutions ranging from 8×8 to 128×128. The L_2 norm of each conserved variable is plotted as a function of grid spacing (relative to the finest grid). Results from this case are in Fig. 12. Clearly, the interior scheme is third order, as it should be, and can therefore be considered verified, at least for subsonic flow.

Other Changes

In addition to the above modifications, numerous other fixes and features have gone into the structured solver portion of Wind-US. Several of these are now briefly noted.

The unified nature of the calculation of viscosity proved its worth as two new viscosity models have been added to the code. The first is a model for Nitrogen that was developed for use at AEDC's Tunnel 9 facility. This model uses a standard Sutherland's Law formulation for moderate temperatures and power law forms for both high and low temperature regions:

$$\mu\left(\frac{slugs}{f\,sec}\right) = \begin{cases} 9.226 \times 10^{-7} T^{0.979} & T \leq 227^\circ R \\ \frac{2.219 \times 10^{-5} T^{\frac{3}{2}}}{T+179.1} & 227^\circ R < T \leq 795^\circ R \\ 6.263 \times 10^{-6} T^{0.659} & T > 795^\circ R \end{cases}$$

The second model allows a user to specify coefficients for a Sutherland's Law formulation written in two-coefficient form:

$$\mu\left(\frac{slugs}{f\,sec}\right) = \frac{c_1 T^{\frac{3}{2}}}{T + c_2}$$

For version 5 of Wind, a new algorithm for computing cell areas and volumes was implemented that attempts to detect and account for the presence of solid boundaries in the interior of grids. Unfortunately, this algorithm does not properly account for the presence of chimera grids embedded within a zone. In addition, it appears to cause difficulties on 2-D axisymmetric grids. For this reason, an option was added to enable the user to activate the more straightforward volume and area algorithm from version 4 (and prior versions).

The Geometric Conservation Law is needed to ensure that conserved variables are properly handled when the computational grids are in motion. This algorithm has now been implemented throughout the structured side of the Wind-US code.

Wind has had a "dq limiter" for some time now, but this limiter acts by decreasing the time step throughout an entire zone whenever it detects a problem. Other codes use a less restrictive algorithm that affects onlythe points at which problems are found. Thinking that such an algorithm might be useful in Wind-US, the investigator implemented the"localdqlimiter"from the NXAIR code.

Several changes have been made to Wind-US's methods of computing the properties of flows with multiple chemical species. Previously, when specifying thermodynamic properties of a chemical specie, it was only possible to have a single temperature range. Now, if needed, different coefficients can be specified for multiple temperature ranges. Also, in the past, there were incompatibilities in the computation of reaction rates that meant that only reaction sets using the old NASA Lewis curve fits would work properly. SPARK curve fits would not function properly, and the newer NASA format was completely unsupported. Now, all three formats are supported, but an extra line is required in the chemistry file to tell the code which format is to be used.

Finally, in the course of development, several algorithms which had previously been advertised as functional were found to be broken (and then fixed). Among these is the ability to use overlapping grids with fringes more than

two deep, which is necessary when running the fourth or fifth order schemes and attempting to preserve the order at boundaries between zones. Also, the simple screen model was repaired, an improved algorithm for the inter-zonal communication of turbulence model variables was implemented, and wall temperatures specified with the "tmptrn" utility now work properly.

Conclusions

Significant improvements have been made to the Wind flow solver, greatly enhancing its stability and applicability to a broad range of simulations, particularly unsteady flows. These additions and fixes have been demonstrated on simple test cases and are now either already being used at AEDC for production work or are undergoing further tests with the aim of transitioning them to production and eventual inclusion in the official version of Wind to released by the NPARC Alliance through the Internet Version Management System.

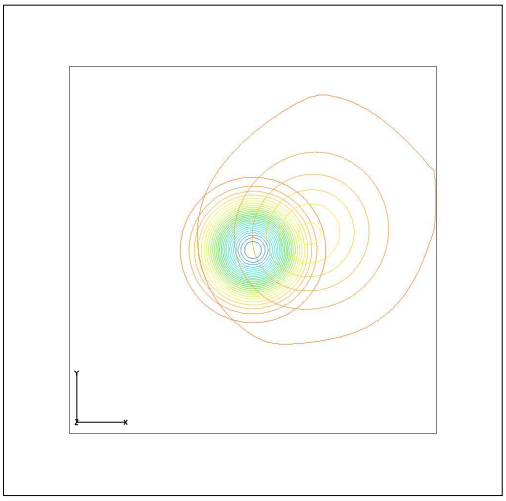

Figure 1. Initial and Final Density Contours from an Inviscid Vortex Convection Simulation using First-order Time- marching

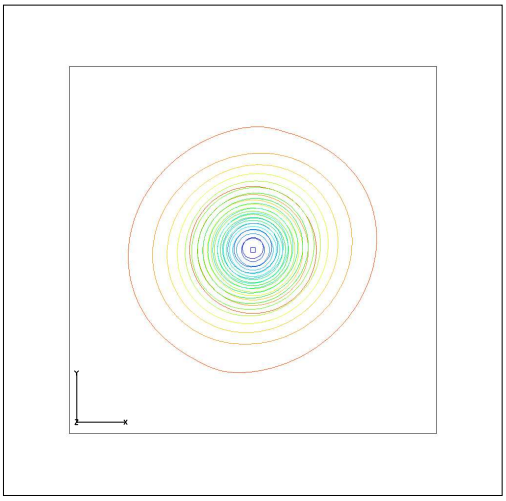

Figure 2. Initial and Final Density Contours from an Inviscid Vortex Convection Simulation using First-order Time-marching with Newton Iteration

References

[1] Bush, R. H., Power, G. D. , and Towne, C. E. WIND: The Production Flow Solver of the NPARC Alliance. AIAA Paper 98–0935, 1998.

[2] Bush, R. H., A Three Dimensional Zonal Navier-Stokes Code for Subsonic through Hypersonic Propulsion Flowfi elds. *AIAA-88-2830*, 1988.

[3] Power, G. D., and Underwood, M.L., WIND 2.0- Progress on an Applications-oriented CFD code. AIAA Paper 99–3212, 1999.

[4] Nelson , C . C . and Power, G. D., CHSSI Project CFD-7: The NPARC Alliance Flow Simulation System. AIAA Paper 2001–0594, 2001.

[5] Lankford, D. W., and Nelson, C.C., Application of the Wind Flow Solver to Chemically Reacting Flows. *AIAA-2002-0673*, 2002.

[6] Nichols, R., and Tramel ,R., Applications of a Highly Effi cient Numerical Method for Overset-mesh Moving Body Problems. AIAA Paper 97–2255, 1997.

[7] Jesperson, D. and Pulliam, T., Recent Advancements to OVERFLOW. *AIAA 97-0644*, 1997.

[8] Spalart, P . R . , Jou, W . H . , Strelets, M . and Allmaras, S.R., Comments on the Feasibility of LES for Wings and on a Hybrid RANS/LES Approach. In *Advances in DNS/LES- Proceedings of the First AFOSR International Conference on DNS/LES*, 1997.

[9] Bush, R.H., and Mani, M., A Two-Equation Large Eddy Stress Model for High Sub-Grid Shear. AIAA Paper 2001–2561, 2001.

[10] Nichols , R . H . , and Nelson, C.C.,Weapons Bay Acoustic Predictions using a Multiscale Turbulence Model. In *Proceedings of the 2001 Aircraft-Store Compatibility Symposium and Workshop*, 2001.

[11] Nelson. C.C., and Nichols, R.H,. Evaluation of Hybrid RANS/LES Turbulence Models using an LES Code. AIAA Paper 2003–3552, 2003.

[12] Nichols, R.H., and Nelson, C.C.,Application of Hybrid RANS/LES Turbulence Models. AIAA Paper 2003–0083, 2003.

[13] Nelson,C. C., and Menon,S.,Unsteady Simulations of Compressible Spatial Mixing Layers. AIAA Paper 98–0786, 1998.

[14] Suzen, Y . B . and Hoffman, K.A.,Investigation of Supersonic Jet Exhaust F l ow by One- and Two-equation Turbulence Models. AIAA Paper 98–0322, 1998.

[15] Eggers,J.M., Velocity Profi les and Eddy Viscosity Distributions Downstream of a Mach 2.22 Nozzle Exhausting to Quiescent Air. Technical Report TN D–3601, NASA, 1966.

[16] Barber,T.J., Chiappetta,L.M., DeBonis, J . R . , Georgiadis, N . J . , and Yoder, D.A.,. An Assessment of Parameters Influencing Prediction of Shear Layer Mixing. *AIAA-97-2639*, 1997.

[17] Buning, P.G., Jespersen, D.C., Pulliam, T.H., Klopfer,G.H., Chan, W.M., Slotnick, J.P., Krist,S.E., and Renze,K.J.,*OVERFLOW User's Manual- Version 1.8q*, August 2000.

[18] Roache, P.J., and Steinberg,S.,Symbolic Manipulation and Computational Fl uid Dynamics. *AIAA Journal*, 22(10):1390–1394, 1984.

[19] Roach, P.J., Knupp,P.M., Steinberg, S., and Blaine,R.L. Experience with Benchmark Test Cases for Groundwater Flow. Celik,I., and Freitas, C . J . , editors, *Benchmark Test Cases for Computational Fluid Dynamics*, number H00598 in ASME FED 93, pages 49–56. 1990.

[20] Oberkampf, W.L., and Blottner, F.G. Issues in Computational Fluid Dynamics Code Verifi cation/Validation. *AIAA Journal*, 36(5):687–695, 1998.

[21] Nelson, C.C., and Roy, C.J., Verifi cation of the Wind-US CFD Code using the Method of Manufactured Solutions. AIAA Paper 2004–1104, 2004.

[22] Hirsch, C.. *Numerical Computation of Internal and External Flows Volume 2: Computational Methods for Inviscid and Viscous Flows*. John Wiley and Sons, 1990.

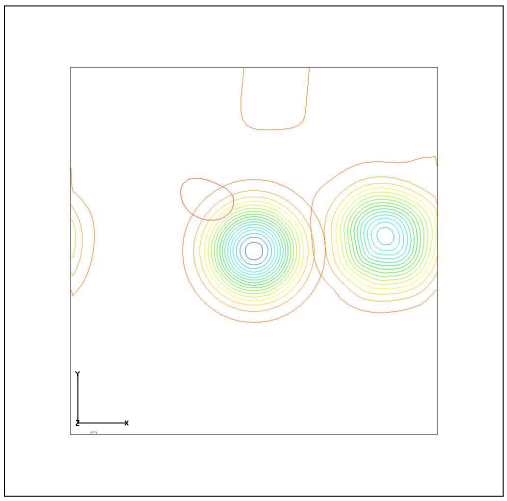

Figure 3. Initial and Final Density Contours from an Inviscid Vortex Convection Simulation using Second - order Time - marching

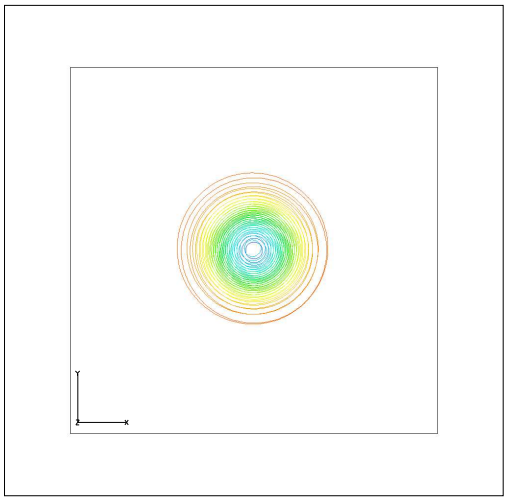

Figure 4. Initial and Final Density Contours from an Inviscid Vortex Convection Simulation using Second-order Time - marching with Newton Iterations

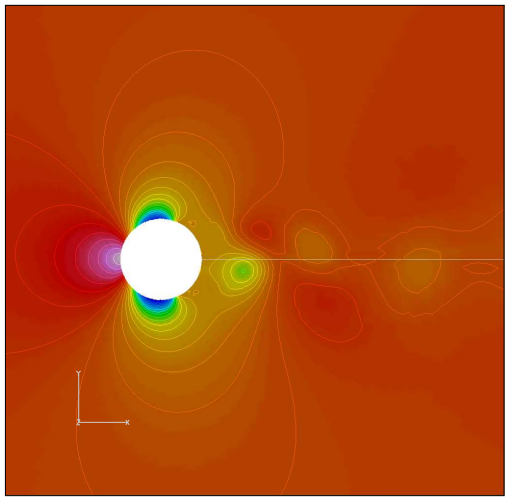

Figure 5. Instantaneous Pressure Contours for a Circular Cylinder at $M = 0.2$ and $Re_d = 8 \times 10^6$ obtained using the Menter SST Turbulence Model

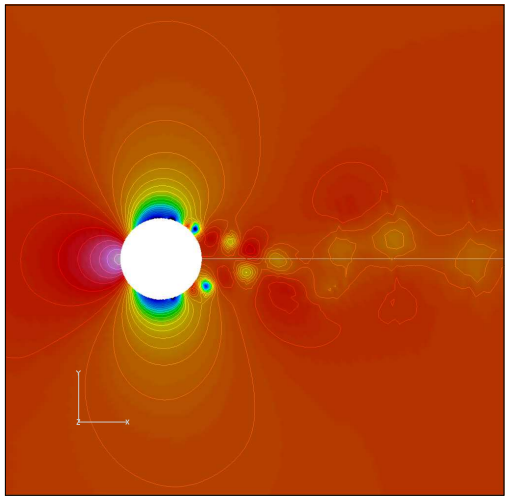

Figure 6. Instantaneous Pressure Contours for a Circular Cylinder at $M = 0.2$ and $Re_d = 8 \times 10^6$ obtained using the Hybrid Technique of Nichols and Nelson Applied to the Menter SST Model

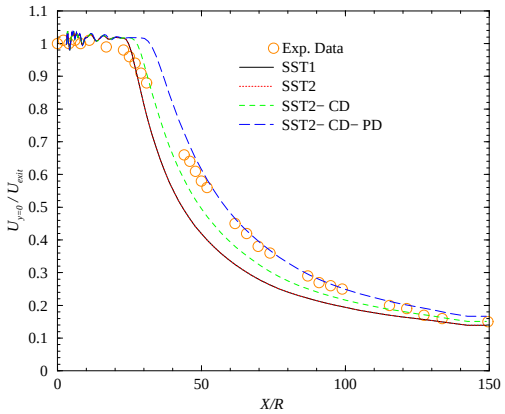

Figure 7. Centerline Axial Velocity in the Nozzle and Plume of an Axisymmetric Free Jet

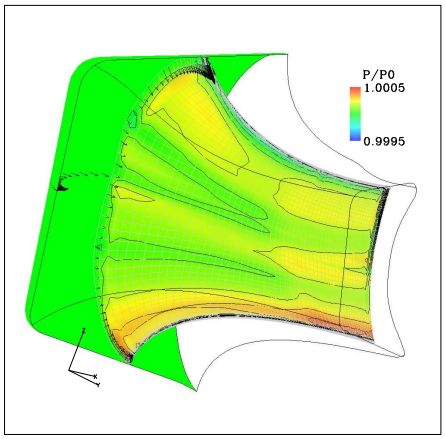

a. Original Wind Infbw Boundary Condition

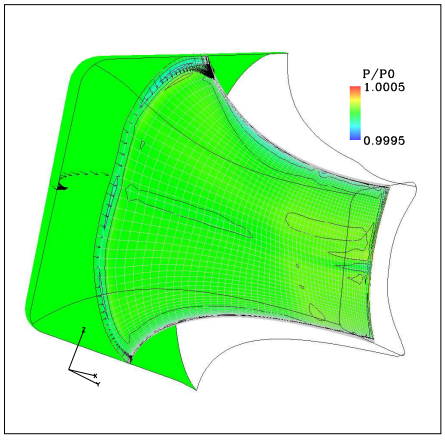

b. Improved Wind-US Infbw Boundary Condition

Figure 8. Normalized Total Pressure Field Variations with Inflow Boundary Condition Treatment

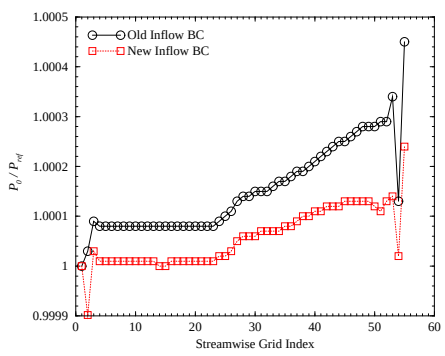

Figure 9. Effect of Inflow Boundary Condition Treatment on Normalized Total Pressure

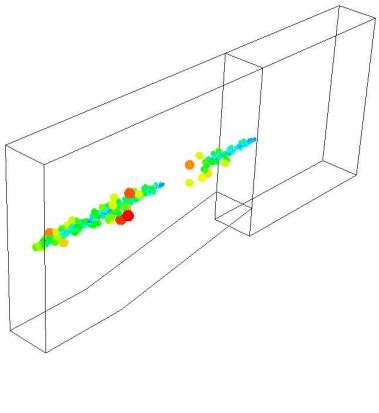

Figure 10. Particle Positions in Zone 1

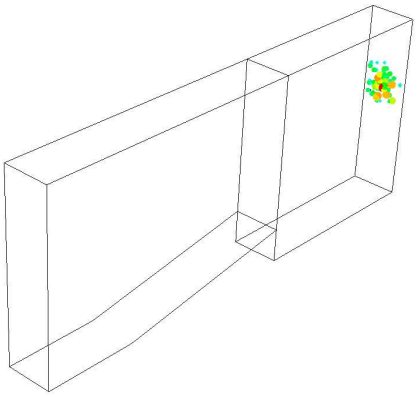

Figure 11. Particle Accumulation at Outflow Boundary

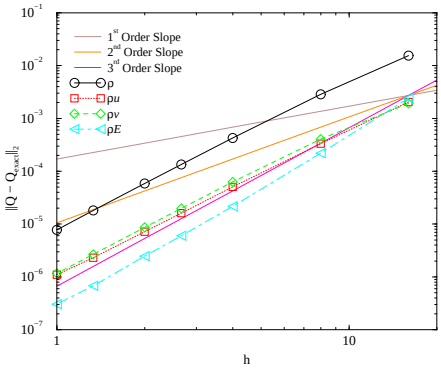

Figure 12. Discretization Error L_2Norm of the Rusanov Scheme obtained using the Method of Manufactured Solutions at Various Grid Resolutions